

Developing a Cylindrical Adjustable Inertance Tube for Pulse Tube Cryocoolers

W.J. Zhou J.M. Pfotenhauer, and G. F. Nellis

Cryogenics Laboratory,
University of Wisconsin - Madison
Madison, WI, USA 53706

ABSTRACT

The length and diameter of the inertance tube play a significant role in achieving the desired phase angle for a pulse tube cryocooler. This paper reports on the design and experimental evaluation of a cylindrical adjustable inertance tube that has the ability to adjust the phase angle of a pulse tube cryocooler in real time during operation. This cylindrical adjustable inertance tube has the ability to change its length from 1.37 m to 2.92 m and to adjust its diameter from 6.9 mm to 8.7 mm while turning the outer screw between its two end positions. Preliminary experimental results demonstrate phase angle shifts from -31.53° to -50° as the frequency increases from 30 Hz to 60 Hz.

INTRODUCTION AND PREVIOUS WORK

The inertance tube (IT) is a significant passive phase shifting device for a Stirling type pulse tube cryocooler. Since it was first introduced by Kanao[1] in 1994, it has become a topic of interest in the cryocooler research field. Various scholars[2-14] have contributed significantly to our understanding of the phase shifting performance of inertance tubes. According to model predictions, the phase angle generated by the inertance tube can be very sensitive to different diameters and lengths[12]. However, in practical applications, typically a long copper or stainless steel tube with a fixed diameter and length is connected to the cryocooler, and it might not provide an optimum phase angle for the specific cryocooler. Thus, another stainless steel tube with a different diameter and length must be tried on the same cryocooler. Such an approach for fixing the optimum phase angle would require a long and complicated process. Therefore, we are pursuing the idea of an adjustable inertance tube (AIT), that can provide a variable length or diameter, or both, in real time while the pulse tube is operating.

In our previous papers, the performance of the linear adjustable inertance tube is detailed and reported [12, 13]. The mass flow and pressure oscillations, as well as the phase angle difference are measured from the experiment, and these match our distributed component model predictions [9]. However, due to the constraints of available length change (less than 20%), the linear adjustable inertance tube provides only a 12° phase angle shift adjustment. Furthermore, even the length change from 1.29 m to 1.53 m proved to be rather awkward in the linear configuration. Because of the above issues, we have proposed conical and cylindrical adjustable inertance tube configurations and have theoretically explored their performance [14]. From the theoretical prediction, the conical

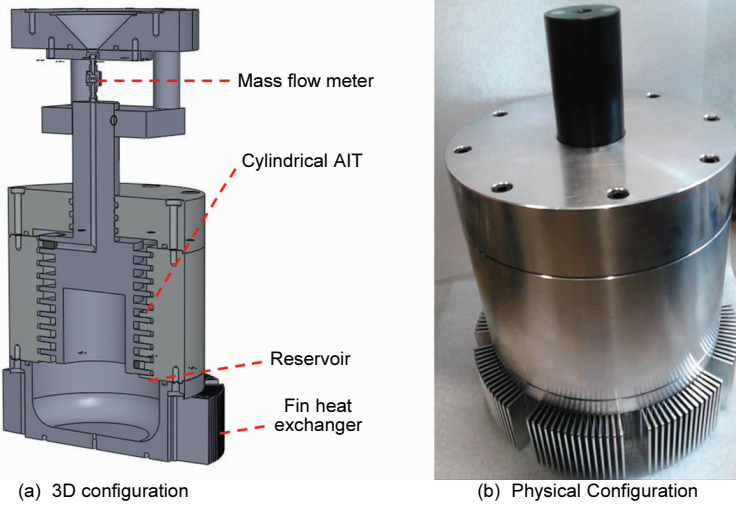


Figure 1. Structure of cylindrical adjustable inertance tube

Table 1. Parameters of cylindrical adjustable inertance tube

| | | | |
|------------------------------------|---------|------------------------------------|---------|
| $D_{\min}(\text{mm})$ | 6.9 | $D_{\max}(\text{mm})$ | 8.7 |
| $L_{\min}(\text{m})$ | 1.37 | $L_{\max}(\text{m})$ | 2.92 |
| $V_{\text{res},\min} (\text{m}^3)$ | 1.42e-3 | $V_{\text{res},\max} (\text{m}^3)$ | 1.59e-3 |
| N (turns) | 4.5 | | |

adjustable inertance tube can only provide a limited phase angle shift, while the cylindrical adjustable inertance tube can not only provide a larger phase angle shift, but also has the ability to maintain a constant acoustic power consumption. Therefore, a cylindrical adjustable inertance tube has been designed, fabricated and tested in order to further explore the phase shifting ability of an adjustable inertance tube. Figure 1 shows a 3-D drawing and photo of the cylindrical adjustable inertance tube. The channel between the two threads of the inner screw and outer screw defines the adjustable inertance tube. By turning the outer screw from its bottommost position (as shown in Fig. 1) to its topmost position, the effective diameter and length decrease from 8.7 to 6.9 mm and from 2.92 to 1.37 m, respectively. The basic parameters of the cylindrical adjustable inertance tube are shown in Table 1. As shown in Figure 1, the cylindrical adjustable inertance tube also includes a circular fin heat exchanger and the reservoir all in one compact package. In the present experiment, the oscillating mass flow rate is measured by the screen pack mass flow meter at the entrance of the inertance tube.

In this paper, we describe the design process and preliminary experimental results from testing the cylindrical adjustable inertance tube. This paper includes four sections including this introduction and previous work. The second section describes the design procedure and some characteristics of the cylindrical adjustable inertance tube. The third section gives some preliminary experimental results that demonstrate its phase shifting ability. The last section summarizes these preliminary experimental results and discusses future work.

DESIGN OF THE CYLINDRICAL ADJUSTABLE INERTANCE TUBE

The cylindrical adjustable inertance tube enables a changing diameter and length for the inertance tube via concentric screws. As shown in Figure 1, the effective diameter and total length vary by turning the outer screw from the bottommost position to the topmost position. A spring-loaded stop located at the top end of the inner screw and another spring-loaded stop on the bottom end of the outer screw define the length of the inertance tube. The bottom stop is fixed to the outer screw,

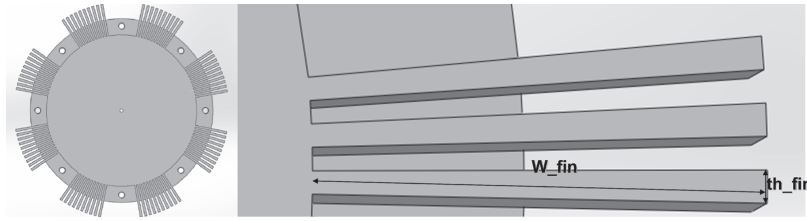


Figure 2. Fins heat exchanger around the reservoir

Table 2. Basic fin design parameters.

| | | | |
|---------------|-------|------------------|-------|
| T_air (K) | 293 | k_fin (W/m-K) | 177 |
| W_fin (m) | 0.102 | th_fin (m) | 0.002 |
| L_fin (m) | 0.038 | Dia_cylinder (m) | 0.178 |
| a_fin (m) | 0.002 | h_fin (W/m^2-K) | 20 |
| q_dot_fin (W) | 300 | N_fin | 68 |

and the top stop is fixed to the inner screw. The bottom stop travels with the outer screw as the outer screw moves up and down, while the top stop remains static with the inner screw. In this way both the length and the diameter increase or decrease at the same time.

The empty chamber attached to the bottom of the outer screw in Figure 1 is the gas reservoir. The volume of this reservoir changes as the position of the inner screw is adjusted. Its volume decreases from 1.59 L to 1.42 L as the outer screw travels from its bottom to its top position. From the model prediction, this amount of volume change has an insignificant influence on the phase angle between the mass flow rate and pressure wave at the inlet of the inertance tube.

There are several fins around the reservoir to cool the temperature of the reservoir during the operation of the pulse tube. An anodized coating is used on the teeth of the inner screws to decrease the friction between the inner and outer screw-threads. A long channel extends from the inlet of the inner screw to the adjustable inertance tube inlet. The diameter is chosen to ensure that the pressure drop along this channel is significantly smaller than the pressure amplitude of the oscillations. Several O-rings are used to seal the 2.0 MPa average pressure inside the inertance tube.

a) Fin Heat Exchanger around the Reservoir

During the operation of a pulse tube refrigerator, there may be a significant amount of acoustic power consumed in the concentric screw configuration. The fin heat exchanger is added on the outside of the reservoir to maintain the temperature below 50°C. Figure 2 shows the detailed dimensions of the fin heat exchanger; it is located around the outside of the reservoir cover and fixed to the outer screw by eight bolts and an O-ring seal.

Table 2 displays the parameters of the finned heat exchanger. The entire adjustable inertance device is fabricated out of aluminum 6061. The fin thickness is 2 mm, with 38 mm length and 102 mm height. As a conservative approach, the fins are designed to reject up to 300 W of acoustic power, close to the amount generated by the linear compressor in the experiment. The surface temperature of the reservoir is thereby designed not to exceed 50°C.

From Figure 3, we can see that if the fin thickness is about 2mm, the surface temperature will be less than 50°C when the acoustic power is about 300 W. The total number of fins around the reservoir is 68 as is shown in Table 2. The reservoir surface temperature decreases as the fin thickness decreases; however, fins thinner than 2 mm are increasingly, and unnecessarily, difficult to fabricate. Therefore, a 2 mm fin thickness is used for the finned heat exchanger.

b) Pressure Drop along the Channel

The long channel, extending from the inlet of the inner screw to the adjustable inertance tube inlet, is shown in Figure 1. If the pressure drop along this channel is as large as the pressure amplitude in the inertance tube, the performance of the adjustable inertance tube will be completely degraded. The pressure drop along this channel is very sensitive to the diameter and length of the

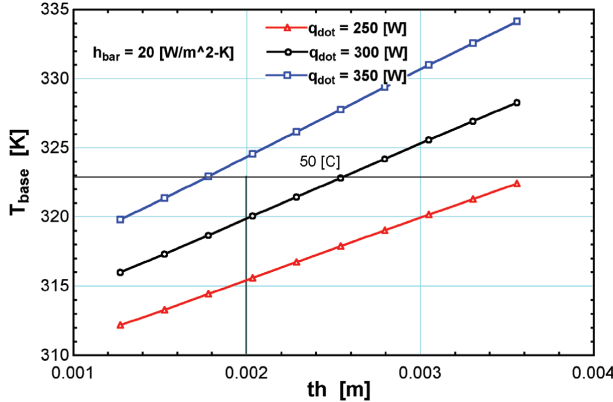


Figure 3. Temperature of the reservoir vs. thickness of the fins

channel. Therefore, the pressure drop along this channel is also calculated to determine the diameter of this channel. The pressure loss is estimated using the steady flow equation:

$$\Delta P = f \cdot \rho \cdot \frac{L}{D_i} \cdot \frac{u_m^2}{2} \quad (1)$$

$$\dot{m} = P_d \cdot 2\pi f \cdot \cos(2\pi ft) \frac{V_{res}}{\gamma R_{he} T_0} \quad (2)$$

In Equation (1), f stands for the friction factor of the pipe, u_m is the bulk velocity of the working fluid, ρ is the density of the helium gas, L is the length of the pipe, and D_i is the inner diameter of the pipe. Equation (2) shows the helium mass flow rate in the inertance tube. P_d stands for pressure amplitude, V_{res} is the volume of the reservoir, γ is the helium specific heat ratio, T_0 is the gas temperature in the inertance tube, and f is the sinusoidal frequency. The helium mass flow rate can change from 0.001 kg/s to 0.005 kg/s in the experiment. By changing the inner diameters of the pipe, the pressure drop is calculated from Equation (1). A key criteria in the design of the inner diameter of the pipe is to make sure that the pressure drop is much smaller than the pressure amplitude of the oscillating flow in the inertance tube.

Figure 4 illustrates the pressure drop versus inner diameter of the pipe at different helium mass flow rates. From the curves in the figure, the calculated pressure drop along a 5 mm diameter channel is about 7189 Pa, which is only 3% of the pressure typical operating amplitude of 228 kPa in the variable inertance tube. Additionally, the 5 mm diameter channel is relatively easy to fabricate and was therefore selected for this design.

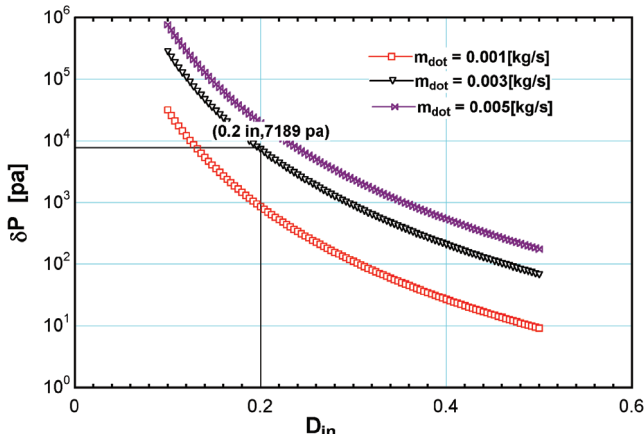


Figure 4. Pressure drop along the channel

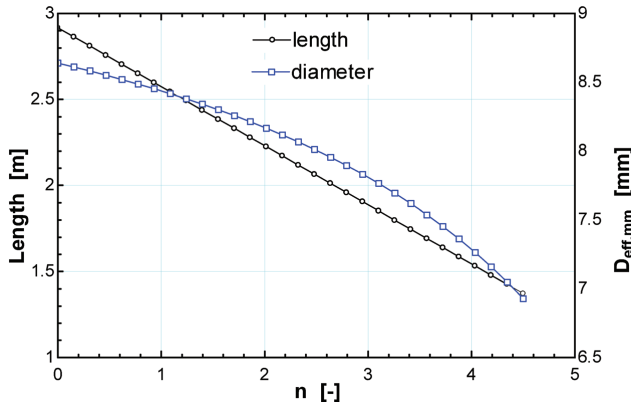


Figure 5. Length and diameter versus number of turns of outer screw

EXPERIMENTAL VERIFICATION

A preliminary experiment has been carried out to measure the performance of the adjustable inertance tube. A linear compressor (Q Drive Model 2S297W) is used to generate the oscillating flow. The mass flow meter is connected between the outlet of the linear compressor and the inlet of the cylindrical adjustable inertance tube. The mass flow meter is constructed by using a six-piece copper screen pack (80 mesh) and two Endevco model B8510B-500 pressure sensors, one on each side of the screen pack [12], as is shown in Figure 1. The inner screw is fixed in place with a flange that is attached to the aftercooler.

The phase angle between the mass flow and pressure oscillations is measured by a Labview Lock-in amplifier program. A Stanford Research SR830 Lock-in amplifier is also used to verify the Labview Lock-in program. Both instruments provide essentially the same phase angle measurement in the experiment. During the operation, the length and diameter is changed by turning the outer screw from the bottom position to the top position. Figure 5 shows the length and diameter change as a function of the number of turns of the outer screw. The cylindrical adjustable inertance tube provides for a maximum of 4.5 turns. As the outer screw moves from the bottommost position to the topmost position, the total length decreases linearly while the effective diameter decreases like a parabolic curve, as shown in Figure 5.

Figure 6 shows the measured phase angle between the mass flow rate and pressure wave at the inlet of the cylindrical inertance tube. The screen pack mass flow meter [12] is implemented to capture the phase angle. The linear compressor is initially set to operate with a charge pressure of 2 MPa and 30 Hz. Figure 6, displays that in these conditions, the mass flow rate leads the pressure

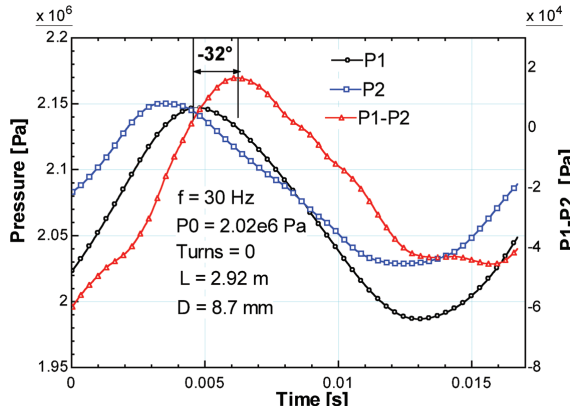


Figure 6. Phase angle between mass flow and pressure in cylindrical inertance tube

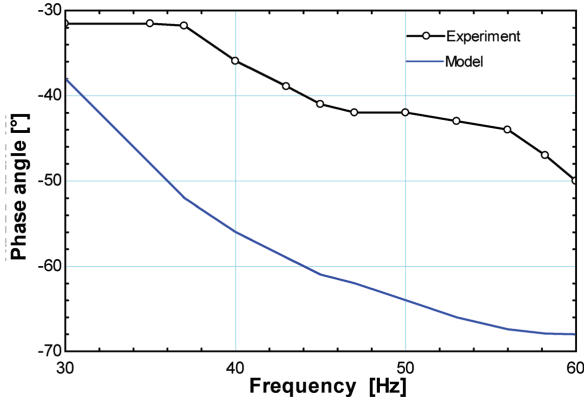


Figure 7. Phase angle shift with the changing frequency in cylindrical inertance tube

wave by almost -32° . At this point, the cylindrical inertance tube is positioned where it has the largest diameter and length. During the initial operation of the experiment, one of the pressure transducers was damaged and subsequently produced unsteady pressure signals. Due to time constraints, only a limited amount of data was obtained, that displaying how the cylindrical inertance tube performed at different frequencies.

Figure 7 shows the change of phase angle with frequency at a charge pressure of 2.06 MPa. The experimental data is also compared with the Distributed Component Model [9]. From the model prediction, as the frequency increases from 30 Hz to 60 Hz, the phase angle will shift from -38° to -68° , almost a 30° phase angle change. From the experiment, the phase angle shifts from -31.53° to -50° .

DISCUSSION AND CONCLUSION

This paper reports on initial measurements using a cylindrical adjustable inertance tube for a Stirling type pulse tube cryocooler. The adjustable inertance tube can change the diameter and length in real time during operation of the pulse tube. The design process addresses the configuration of a finned heat exchanger and the pressure drop between the pulse tube outlet and the entrance of the inertance tube. The cylindrical adjustable inertance tube has also been fabricated and tested in our lab.

The initial experimental results demonstrate a phase angle shift from -31.53° to -50° , as the frequency increases from 30 Hz to 60 Hz. The results are in fairly good agreement with predictions from the Distributed Component Model. Further experiments will be carried out to fully explore the relationship between the adjustable diameter and length of the cylindrical inertance tube and the phase angle shift for the Stirling type pulse tube cryocoolers.

ACKNOWLEDGMENTS

The authors thank Mike Hughes, David Arawinko and Joel Ballweg for many valuable discussions and fabrication of the cylindrical adjustable inertance tube.

REFERENCES

1. Kanao, K.-i., N. Watanabe, and Y. Kanazawa, "A miniature pulse tube refrigerator for temperatures below 100K," *Cryogenics*, 1994, **34** (Supplement 1), pp. 167-170.
2. Zhu S., et al., "Phase shift effect of the long neck tube for the pulse tube refrigerator," *Cryocoolers 9*, Plenum Press, New York (1997), pp. 269-278.
3. Gardner, D.L. and G.W. Swift, "Use of inertance in orifice pulse tube refrigerators," *Cryogenics*, 1997, **37**(2), pp. 117-121.

4. Roach, P.R. and K. A., "Pulse tube coolers with an inertance tube: Theory, Modeling, and Practice," *Adv. in Cryogenic Engineering*, Vol. 43B, Plenum Publishing Corp., NY (1998), pp. 1895-1902.
5. de Boer, P.C.T., "Performance of the inertance pulse tube," *Cryogenics*, 2002. **42**(3-4), pp. 209-221.
6. Swift, G.W., M.S. Allen, and J.J. Wollan, "Performance of a Tapered Pulse Tube," *Cryocoolers 10*, Plenum Publishing Corp., New York (1999), pp. 315-320.
7. Luo, E., R. Radebaugh, and M. Lewis, "Inertance Tube Models and Their Experimental Verification," *AIP Conference Proceedings*, 2004. **710**(1), pp. 1485-1492.
8. Lewis, M.A., et al., "Measurements of Phase Shifts in an Inertance Tube," *Cryocoolers 13*, Springer Science+Business Media, New York (2005), pp. 267-273.
9. Schunk, L.O., G.F. Nellis, and J.M. Pfotenhauer, "Experimental Investigation and Modeling of Inertance Tubes," *Journal of Fluids Engineering*, 2005, **127**(5), pp. 1029-1037.
10. Radebaugh, R., et al., "Inertance Tube Optimization for Pulse Tube Refrigerators," *AIP Conference Proceedings*, 2006, **823**(1), pp. 59-67.
11. Lewis, M.A., et al., "Impedance Measurements of Inertance Tubes at High Frequency and Pressure," *AIP Conference Proceedings*, 2008. **985**(1): pp. 1083-1090.
12. J. M. Pfotenhauer, T. Steiner, and L.M. Qiu., "Continuously Variable Inertance Tubes for Pulse Tube Refrigerators," *Cryocoolers 16*, ICC Press, Boulder, CO (2011), pp. 275-280.
13. W.J. Zhou and J.M. Pfotenhauer, J.M., "Real Time Phase shifting with an Adjustable Inertance Tube," *Cryocoolers 17*, ICC Press, Boulder, CO (2012), pp. 229-238.
14. W. J. Zhou, J.M.P., G. F. Nellis, "Comparison of three adjustable inertance tubes," *Advances in Cryogenic Engineering*, 2013. **1573**(59B), pp. 994-1001.